Analysis of the membrane topology for transmembrane domains 7–12 of the human reduced folate carrier by scanning cysteine accessibility methods

Wei CAO* and Larry H. MATHERLY*†[1]

*Department of Pharmacology, Wayne State University School of Medicine, 540 E. Confield Ave., Detroit, MI 48201, U.S.A., and †Experimental and Clinical Therapeutics Program, Barbara Ann Karmanos Cancer Institute, Wayne State University School of Medicine, 110 E. Warren Ave., Detroit, MI 48201, U.S.A.

The hRFC (human reduced folate carrier) is the major membrane transporter for both reduced folates and antifolates in human tissues and tumours. The primary amino acid sequence of hRFC predicts a membrane topology involving 12 TMDs (transmembrane domains) with cytosolic oriented N- and C-termini, and a large internal loop connecting TMDs 6 and 7. Previous studies using haemagglutinin epitope insertion and scanning glycosylation mutagenesis methods verified portions of the predicted topology model, including TMDs 1–8 and the N- and C-termini of hRFC. However, the topology structure for TMDs 9–12 remains controversial. To further determine the membrane topology of the hRFC protein, single cysteine residues were introduced into the predicted extracellular or cytoplasmic loops of a fully functional cysteine-less hRFC expressed in transport impaired MtxRIIOua^{R}2-4 Chinese hamster ovary cells. The membrane orientations of the substituted cysteines were determined by treatments with the thiol reagents 3-(*N*-maleimidylpropionyl)-biocytin (biotin maleimide) and 4-acetamido-4′maleimidylstilbene-2,2′-disulphonic acid (stilbenedisulphonate maleimide; SM) or *N*-ethylmaleimide, combined with the cell-permeabilizing reagent SLO (streptolysin O). We found that cysteine residues placed in the predicted extracellular loops between TMDs 7 and 8 (position 301), 9 and 10 (360), and 11 and 12 (429) could be biotinylated with 200 μM biotin maleimide, and labelling could be blocked with SM. However, biotinylation of cysteines placed in the predicted intracellular loops between TMDs 8 and 9 (position 332) and TMDs 10 and 11 (position 388) was only detected after cell permeabilization with SLO and was abolished by pre-treatment with *N*-ethylmaleimide. These results strongly support a 12-TMD topology structure for the hRFC protein.

Key words: folate, 3-(*N*-maleimidylpropionyl)-biocytin, membrane topology, methotrexate, transmembrane domain, transporter.

INTRODUCTION

The ubiquitously expressed RFC (reduced folate carrier) is the major transport system for reduced folates and classical antifolates in mammalian cells [1–4]. For reduced folates such as 5-methyl and 5-formyl tetrahydrofolate, adequate rates of intracellular delivery are essential for DNA synthesis and cell proliferation. For antifolates such as Mtx (methotrexate), the level of RFC is a major determinant of antitumour activity in cultured tumour cells [3,4] and impaired transport is a frequent mechanism of antifolate resistance in tumour models both *in vitro* [5–10] and *in vivo* [11]. A number of other antifolate chemotherapy drugs (e.g. Pemetrexed, Tomudex) are also excellent substrates for RFC [4,12]. The clinical importance of RFC in cancer chemotherapy was strongly implied by reports of proportional changes in RFC transcripts and Mtx uptake for B-precursor acute lymphoblastic leukaemia lymphoblasts [13,14] and in osteosarcomas from patients [15]. In osteosarcomas, losses of Mtx transport were associated with a poor prognosis [15].

hRFC (human reduced folate carrier) cDNAs were cloned in 1995 [16–19]. By hydropathy analysis [20] of the predicted amino acid sequence, hRFC is predicted to be an integral membrane protein with up to 12 stretches of mostly hydrophobic, α-helix-promoting amino acids, with a large central linker connecting the predicted TMDs (transmembrane domains) 1–6 and TMDs 7–12, internally oriented N- and C-terminal domains, and an external N-glycosylation site at Asn-58 (Figure 1).

A number of studies have shed light on the membrane topological structure of the hRFC protein. For instance, our finding of N-glycosylation of hRFC confirmed an extracellular orientation of Asn-58 (located in TMD2 in Figure 1) [21]. By HA (haemagglutinin) insertional mutagenesis and analysis of functional proteins, extracellular orientations were confirmed for the loops connecting TMDs 3 and 4, 5 and 6, and 7 and 8, and internal orientations were demonstrated for the loops connecting TMDs 4 and 5, 6 and 7, and 8 and 9, and for the N- and C-termini [22,23]. By N-glycosylation scanning mutagenesis, in which N-glycosylation consensus sequences [NX(S/T)] were inserted into putative loop domains, the TMD 5/6 loop sequence was, likewise, confirmed to be extracellular [23]. However, results for TMDs 9–12 and connecting loop domains were ambiguous or inconclusive. This reflects the complete loss of transport activity for hRFCs mutated in these regions and, for the N-glycosylation mutants, an inability to distinguish a lack of glycosylation at inserted N-glycosylation consensus sites due to their cytosolic orientations from effects of spacial constraints that limit their accessibilities to oligosaccharyl transferase [24].

Our recent expression of an epitope-tagged 'cysteine-less' hRFC (hRFC$^{myc-his6}$*Cys-less*) in transport-impaired CHO (Chinese hamster ovary) cells [25] suggested an alternative approach for topology mapping the carrier that would circumvent the limitations of our earlier methods. We describe herein the use of SCAM (scanning cysteine accessibility methods) for establishing the membrane topology of TMDs 7–12 and their connecting

Abbreviations used: hRFC, human reduced folate carrier; TMD, transmembrane domain; Mtx, methotrexate; HA, haemagglutinin; CHO, Chinese hamster ovary; SCAM, scanning cysteine accessibility methods; SLO, streptolysin O; NEM, *N*-ethylmaleimide.

[1] To whom correspondence should be addressed, at the Experimental and Clinical Therapeutics Program (e-mail matherly@karmanos.org).

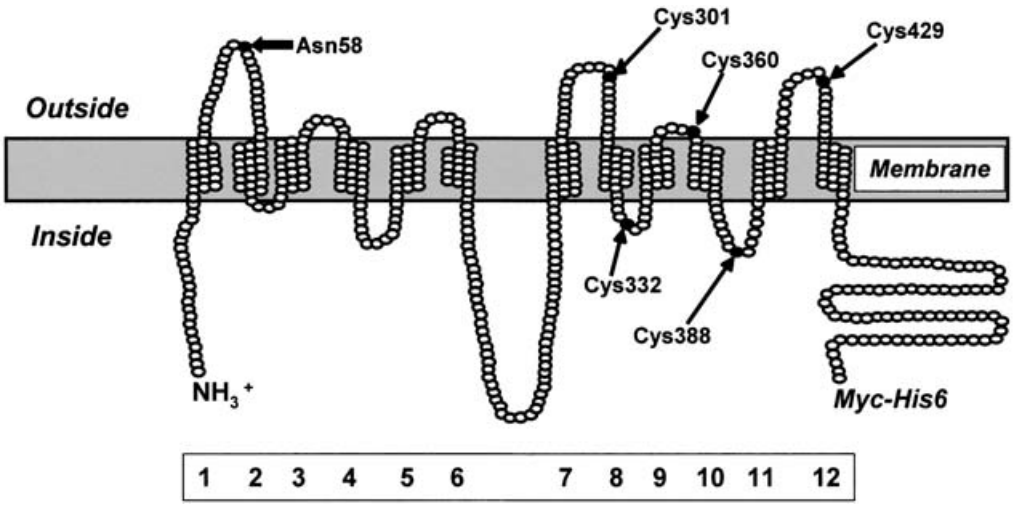

Figure 1 Membrane topology of hRFC and the location of the cysteine insertions

A topology model is shown for the Myc-His6-tagged hRFC protein without the C-terminal 56 amino acids. It depicts 12 TMDs, internally oriented N- and C-termini and TMD 6–7 loop domain, and an externally facing N-glycosylation site at Asn-58. Also shown are the positions of the cysteine residues inserted into the predicted extracellular and cytosolic loops of the hRFC$^{myc-his6}$*Cys-less* protein from TMDs 7–12, as described in the text.

loops, involving insertion of individual cysteine residues into each of the predicted extracellular and intracellular loops of hRFC$^{myc-his6}$*Cys-less* that can then be probed with thiol-reactive maleimide agents. Major advantages of SCAM include the high-level expression of functional single cysteine mutants, reflecting minimal structural effects resulting from cysteine insertions, and a remarkable capacity to unambiguously establish sidedness of inserted cysteines through the use of maleimide reagents differing in membrane permeabilities and the cell-permeabilization reagent, SLO (streptolysin O). Our findings complement earlier studies of hRFC topology [22,23] and, in combination with these prior results, they unequivocally establish a 12-TMD topological structure for hRFC.

MATERIALS AND METHODS

Reagents

[3′,5′,7-^{3}H]Mtx (20 Ci/mmol) was purchased from Moravek Biochemicals (Brea, CA, U.S.A.). Unlabelled Mtx was provided by the Drug Development Branch, National Cancer Institute, Bethesda, MD, U.S.A. Both labelled and unlabelled Mtx were purified prior to use, as described previously [26]. 3-(*N*-Maleimidylpropionyl)-biocytin (biotin maleimide) and 4-acetamido-4′maleimidylstilbene-2,2′-disulphonic acid (stilbenedisulphonate maleimide) were purchased from Molecular Probes (Eugene, OR, U.S.A.). NEM (*N*-ethylmaleimide) was purchased from Sigma Chemical Company (St. Louis, MO, U.S.A.). Protein G-plus Agarose beads were purchased from Santa Cruz Biotechnology (Santa Cruz, CA, U.S.A.). Restriction enzymes and other molecular biologicals were from Promega (Madison, WI, U.S.A.), Invitrogen (Carlsbad, CA, U.S.A.) or Roche (Indianapolis, IN, U.S.A.). Tissue culture reagents and supplies were purchased from assorted vendors with the exception of iron-supplemented calf serum and dialysed fetal bovine serum, which were purchased from Hyclone Technologies (Logan, UT, U.S.A.) and Life Technologies (Gaithersburg, MD, U.S.A.), respectively. Synthetic oligonucleotides were purchased from Invitrogen. SLO was obtained from Dr Sucharit Bhakdi (University of Mainz, Mainz, Germany).

Table 1 PCR primers for preparing single-cysteine-substituted hRFC mutant constructs

Mutation	Sense primer (5′ → 3′)	Antisense primer (5′ → 3′)
S301C	CCACCAACTGTGCGCGTGTCTAC	GTAGACACGCGCACAGTTGGTGG
A332C	CCGCTGGTGTCGCTGGTCTAAG	CTTAGACCAGCGACACCAGCGG
S360C	CACCCGTGTAGTATCTGGCTG	CAGCCAGATACTACACGGGTG
A388C	CCTTTCAAATTTGCTCTTCTCTGTC	GACAGAGAAGAGCAAATTTGAAAGG
R429C	CTCCCGGTTTGCAAGCAGTTC	GAACTGCTTGCAAACCGGGAG

Cell culture

Transport-defective Mtx-resistant CHO cells, MtxRIIOua^{R}2-4 [27], were a gift of Dr Wayne Flintoff (University of Western Ontario, London, Ontario, Canada). MtxRIIOua^{R}2-4 cells were grown in α-minimal essential medium with 10% iron-supplemented bovine calf serum, penicillin (100 units/ml) and streptomycin (100 μg/ml). hRFC$^{myc-his6}$*Cys-less* and hRFC$^{myc-his6}$*wt* transfectants were derived from MtxRIIOua^{R}2-4 cells, as described previously [25], and maintained in complete medium in the presence of 1.5 mg/ml G-418.

Site-directed mutagenesis

A 'wild-type' hRFC construct (designated hRFC$^{myc-his6}$*wt*), containing a truncated open reading frame encoding 7 of the 11 cysteines, and including both c-*myc* and hexahistidine epitopes at the C-terminus, was prepared by subcloning 1607 bp of hRFC coding sequence into pcDNA3.1 (−) myc-his A expression vector (Invitrogen) at the *Bam*HI and *Xho*I restriction sites [25]. The hRFC$^{myc-his6}$*Cys-less* construct, in which all cysteines were replaced by serines, was prepared from hRFC$^{myc-his6}$*wt* by a PCR overlap-extension mutagenesis method [25].

hRFC$^{myc-his6}$*Cys-less* in pCDNA3.1 was used as the template for overlap-extension PCR to generate single cysteine mutant hRFCs. The complementary mutagenesis primers used to construct the cysteine mutants are listed in Table 1. The forward and reverse mutagenesis primers were paired with antisense (CW9,

5′-GGGCCAGGTATGGGTCGCTCTGTCTCTG-3′; positions 1674–1647) and sense (KS2, 5′-CGCAGCCTCTTCTTCAAC-CGC-3′; positions 622–642) hRFC primers, respectively. PCR conditions for the primary PCRs were 94 °C for 30 s, 58 °C for 30 s and 72 °C for 45 s. Secondary PCRs were performed under the same conditions with the KS2/CW9 primers and the mixed primary PCR products as templates. The mutant amplicons were digested with *Not*I and *Sfi*I and ligated into *Not*I/*Sfi*I-digested hRFC$^{myc-his6}$*Cys-less* in pCDNA3.1 to generate S301C, A332C, S360C, A388C and R429C hRFC$^{myc-his6}$ constructs. All constructs were confirmed by automated sequencing at the Center of Molecular Genetics sequencing facility at Wayne State University, Detroit, MI, U.S.A.

Cell transfections and selection of stable transfectants

hRFC$^{myc-his6}$ constructs in pCDNA3.1 (5 μg) were transfected into transport-defective MtxRIIOua^{R}2-4 CHO cells with polybrene [16,25]. Clones were selected with G-418 (1.5 mg/ml) and G-418-resistant clones were isolated and expanded. Stable transfectants were initially screened for Mtx sensitivities by plating at low densities (10000 cells/ml) in complete medium with dialysed fetal bovine serum and 0, 10, 50 or 200 nM Mtx. Clones exhibiting restored Mtx sensitivities compared with MtxRIIOua^{R}2-4 cells were assayed for [^{3}H]Mtx uptake (see below) and hRFC expression on Western blots [7,16,25].

Transport assays

Uptakes of [^{3}H]Mtx (0.5 μM) were measured over 10 min, as described previously [25]. Levels of intracellular radioactivity were expressed as pmol/mg protein, calculated from direct measurements of radioactivity and protein contents of cell homogenates. Protein assays were performed by the method of Lowry et al. [28].

Biotinylation of intact cells, immunoprecipitations and Western blot analysis

CHO transfectants (1×10^{7} cells), growing on 100 mm dishes expressing hRFC$^{myc-his6}$*Cys-less* and the S301C, A332C, S360C, A388C and R429C single-cysteine-substituted hRFC$^{myc-his6}$ mutants, were washed three times with Dulbecco's PBS. Cells were preincubated in PBS without additions or with stilbenedisulphonate maleimide (200 μM, in PBS) at room temperature for 30 min, washed three times with PBS, and then biotinylated by incubation with biotin maleimide (200 μM, in PBS) at room temperature for 30 min. Biotin maleimide was added from a stock solution prepared in DMSO. The concentration of DMSO in the labelling buffer did not exceed 1 % (v/v). After incubation, cells were briefly treated with 2-mercaptoethanol (14 mM) to remove excess reagent and then washed twice with PBS. Cells were harvested and plasma membranes prepared as described previously [29]. For immunoprecipitation, membrane proteins were solubilized in 1 ml of cell lysis buffer (50 mM Tris, pH 7.5, 150 mM NaCl, 1 % Nonidet P40 and 0.5 % sodium deoxycholate). Insoluble material was pelleted (12000 ***g***, 10 min) and the supernatant was precleared for at least 3 h at 4 °C with Protein G-plus Agarose beads. The beads were again pelleted (12000 ***g***, 20 s), and the supernatant was incubated with anti-Myc antibody (Invitrogen) and fresh Protein G-plus Agarose beads overnight at 4 °C. The beads were washed five times with lysis buffer with 0.1 % Nonidet P-40, and eluted with 40 μl of Laemmli sample buffer [30] containing 2 % SDS. Immunoprecipitated proteins were fractionated on SDS/polyacrylamide gels [30] and electrotransferred to PVDF membranes [31]. Immunodetection of biotinylated hRFC was with peroxidase-linked streptavidin (Roche) and Lumi-Light^{PLUS} substrate (Roche), whereas total immunoprecipitated hRFC was detected with hRFC-specific antibody [7] with standard Lumi-Light substrate (Roche).

To label internal cysteines with biotin maleimide, cells (in 100 mm culture dishes) were washed twice with cold PBS. Subsequently, 3 ml of PBS with or without stilbenedisulphonate maleimide (SM, 200 μM) or NEM (3 mM) was used to pretreat the cells at room temperature (for 30 and 5 min, respectively). Cells were then washed three times with cold PBS and permeabilized by treatment with 0.5 μg/ml SLO [32,33]. For permeabilization, cells were washed once with ice-cold incubation buffer (20 mM Hepes, pH 7.2, 140 mM potassium glutamate, 5 mM EGTA, 5 mM $MgCl_2$ and 5 mM NaCl), and then incubated with 0.5 μg/ml SLO in 3 ml of incubation buffer for 10 min at 4 °C. Cells were washed once with ice-cold incubation buffer, then incubated for 20 min at 37 °C in 3 ml of incubation buffer containing 1 mg/ml BSA and 1 mM dithiothreitol. Permeabilized cells were washed with PBS and treated with biotin maleimide (200 μM), followed with membrane preparation and immunoprecipitation, as described above.

RESULTS AND DISCUSSION

Construction and functional assays of single cysteine hRFC mutants in the TMD 7–12 loop domains

A computer-generated topology model (TMPRED) [20] based on the predicted hRFC amino acid sequence is shown in Figure 1. In this model, hRFC is depicted as an integral membrane protein with 12 TMDs, with TMDs 1–6 and 7–12 linked by a large cytosolic connecting loop, and with cytosolic oriented N- and C-temini. Portions of this model (i.e. TMDs 1–8 and the N- and C-termini) have been experimentally verified by HA epitope insertion and glycosylation scanning mutagenesis methods [21–23]. However, these methods could not convincingly establish the topology structure for TMDs 9–12 due to inherent limitations. For instance, for HA epitope accessibility methods, insertion of the 9 amino acid HA epitope did not appreciably affect plasma membrane targeting; however, many of the epitope-tagged proteins were functionally inactive [22,23], presumably due to protein misfolding and/or the assumption of conformational states different from wild-type carrier. For glycosylation scanning mutagenesis, glycosylation status by Western blotting was used to identify extracellularly oriented domains; however, this method was not useful for unequivocally identifying cytosol-oriented domains [23].

In our previous study, we constructed a cysteine-less hRFC, in which all cysteine residues were mutagenized to serines [25]. Functional hRFC$^{myc-his6}$*Cys-less* protein was expressed at high levels in transport-impaired MtxRIIOua^{R}2-4 CHO cells and exhibited normal plasma membrane targeting and similar transport properties to the wild-type hRFC$^{myc-his6}$*wt* protein. Based on prior topology studies of p-glycoprotein [34] and the glutamate transporter GLT-1 [35], it seemed reasonable to use our cysteine-less hRFC construct with SCAM and thiol-reactive agents to further explore the topological structure for the putative TMDs 7–12 in hRFC.

Accordingly, we used hRFC$^{myc-his6}$*Cys-less* as a template to generate a series of cysteine insertion hRFC mutants, with single cysteine residues inserted into each of the putative extracellular or intracellular loop domains for TMDs 7–12 (S301C, A332C, S360C, A388C and R429C, shown in Figure 1). Mutant hRFC

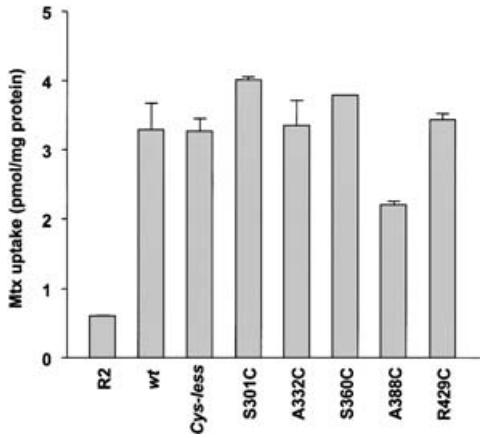

Figure 2 Transport function of single-cysteine-substituted hRFC mutants

Results are shown for [^{3}H]Mtx uptake in MtxRIIOua^{R}2-4 cells (labelled R2) and R2 transfectants expressing hRFC$^{myc-his6}$*wt* (wt) and hRFC$^{myc-his6}$*Cys-less* (Cys-less), and the single-cysteine-substituted hRFC mutants. [^{3}H]Mtx (0.5 μM) uptakes were measured for 10 min at 37 °C. All transport results are means $\pm$ S.E.M. from 2–3 separate experiments.

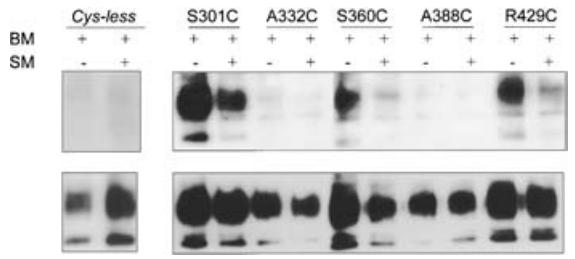

Figure 3 Biotinylation of cysteine-less and single-cysteine-substituted hRFC mutants with biotin maleimide

MtxRIIOua^{R}2-4 transfectants expressing hRFC$^{myc-his6}$*Cys-less* and single-cysteine-substituted hRFC proteins were treated with 200 μM biotin maleimide (BM), with or without pretreatment with 200 μM stilbenedisulphonate maleimide (SM). Membrane proteins were immunoprecipitated by anti-Myc antibody and Protein G-plus Agarose beads, and analysed by Western blotting. Detection of immunoprecipitated proteins used a streptavidin-peroxidase conjugate (upper panels) and hRFC-specific antibody (lower panels), after stripping the PVDF membrane with 0.2 M NaOH.

constructs were transfected into MtxRIIOua^{R}2-4 CHO cells; clones were isolated and screened by cytotoxicity assays from 0 to 200 nM Mtx. Stable transfectants expressing high levels of S301C, A332C, S360C, A388C and R429C hRFCs were confirmed on Western blots (results not shown) and by direct assays of [^{3}H]Mtx uptake. As shown in Figure 2, all the single cysteine mutants displayed 5–8-fold-increased [^{3}H]Mtx uptake over the low levels in MtxRIIOua^{R}2-4 cells and were essentially identical to the wild-type hRFC$^{myc-his6}$*wt* construct. Thus folding and membrane targeting did not seem to be adversely affected by the insertion of the single cysteine residues into the loop domains, suggesting retention of a native protein conformation identical to the wild-type carrier.

Determination of topology for TMDs 7–12 by SCAM

To establish the topological structure for TMDs 7–12 of hRFC, transfected cells expressing S301C, A332C, S360C, A388C and R429C hRFC$^{myc-his6}$ were treated for 30 min with the thiol-reactive agent, biotin maleimide (200 μM), with and without the membrane-impermeant stilbenedisulphonate maleimide (200 μM). Membrane proteins were solubilized, and the c-Myc-tagged hRFC proteins were immunoprecipitated with anti-Myc monoclonal antibody. The immunoprecipitates were fractionated on SDS gels, and the covalently bound biotin was detected with peroxidase-linked streptavidin. Total hRFC proteins were detected on the same blot with anti-hRFC polyclonal antibody [7].

As shown in Figure 3, no biotinylation signal could be visualized for hRFC$^{myc-his6}$*Cys-less*, although a substantial amount of hRFC protein was detected in the immunoprecipitate with hRFC antibody. Consistent with previous HA-insertion mutagenesis results for the TMD 7–8 connecting loop that established its extracellular orientation [22,23], S301C-hRFC$^{myc-his6}$ was highly reactive towards biotin maleimide and labelling was significantly blocked with membrane-impermeant stilbenedisulphonate maleimide [34]. Thus the extracellular cysteine at position 301 is readily accessible to both of the thiol-reactive agents. Conversely, no biotinylation signal was detected with A332C hRFC$^{myc-his6}$ under identical experimental conditions. This implies that the cysteine insertion at position 332 is completely inaccessible to biotin maleimide, perhaps due to the size of the reagent and/or the reducing environment in the cytosol mileau. This lack of reactivity under conditions that readily label extracellular cysteines directly supports the notion of a cytosolic orientation for the TMD 8–9 connecting loop, suggested previously by our HA-accessibility results [23].

Biotin maleimide labelling was extended to determining the orientations of the connecting loops for TMDs 9–10, 10–11 and 11–12, corresponding to the S360C, A388C and R429C hRFC$^{myc-his6}$ constructs, respectively. The S360C and R429C hRFC$^{myc-his6}$ proteins were effectively labelled with biotin maleimide and, in both cases, reactivity was significantly decreased by pretreatment with equimolar stilbenedisulphonate maleimide (Figure 3). Thus the TMD 9–10 and TMD 11–12 loop regions must have an extracellular orientations. However, the result with A388C, located in the TMD 10–11 connecting loop, was inconclusive since no labelling was detected, in spite of high levels of total hRFC protein in the immunoprecipitate (Figure 3).

Although the results in Figure 3 suggest that biotin maleimide exhibits minimal membrane permeability during exposure to 200 μM reagent, a previous study showed that permeabilization with SLO can facilitate labelling of internal cysteines [35]. Accordingly, we treated cells expressing mutant constructs with the cysteine insertions localized to the loop domains for TMD 8–9 (A332C) and TMD 10–11 (A388C), predicted to face the cytosol, with SLO (0.5 μg/ml), prior to treatment with biotin maleimide. Cells were pretreated with stilbenedisulphonate maleimide before incubation with SLO to further verify cysteine accessibilities in the absence of permeabilization. Parallel incubations were performed with the S301C hRFC$^{myc-his6}$ and hRFC$^{myc-his6}$*Cys-less* transfectants. Membrane proteins were immunoprecipitated as before, and levels of total hRFC and biotinylated hRFC proteins were analysed by immunoblotting. High levels of hRFC proteins were detected in the immunoprecipitates for all the transfectants (Figure 4). Predictably, biotin maleimide labelling was negligible for hRFC$^{myc-his6}$*Cys-less*. For S301C hRFC$^{myc-his6}$, a high level of labelling was again detected. In striking contrast to the experiment shown in Figure 3, when cells were permeabilized with SLO, the A332C and A388C hRFC$^{myc-his6}$ mutants were all effectively labelled with biotin maleimide. Since these cysteines were not accessible to stilbenedisulphonate maleimide during the pretreatment interval, no competition for labelling was observed with this reagent (Figure 4A). However, labelling

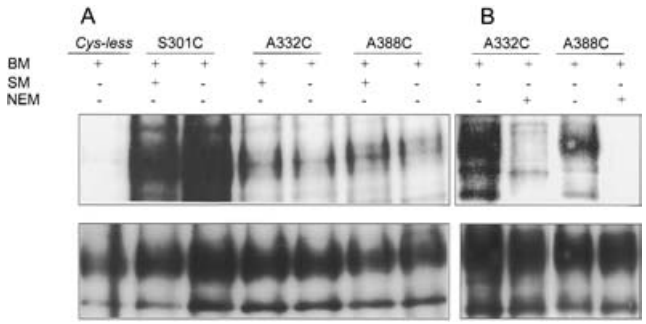

Figure 4 Biotinylation of cytosol-oriented cysteines with biotin maleimide following treatment with SLO

MtxRIIOua^{R}2-4 transfectants expressing hRFC$^{myc-his6}$ *Cys-less* and single-cysteine-substituted hRFC proteins (S301C, A332C, A388C) were incubated with 200 μM stilbenedisulphonate maleimide (SM; **A**) or 3 mM NEM (**B**), washed with PBS, then permeabilized with SLO, as described in the Materials and methods section. Cells were then treated with 200 μM biotin maleimide (BM), and membrane proteins were immunoprecipitated by anti-Myc antibody and Protein G-plus Agarose beads, followed by Western blotting. Detection of immunoprecipitated proteins used a streptavidin-peroxidase conjugate (upper panels) and hRFC-specific antibody (lower panels), after stripping the PVDF membrane with 0.2 M NaOH.

was abolished for A332C and A388C hRFC$^{myc-his6}$ upon pre-treatment with the membrane-permeable reagent NEM (Figure 4B). Collectively, these results clearly demonstrate cytosolic orientations for the TMD 8–9 and TMD 10–11 connecting loops.

Conclusions

In conclusion, we have used SCAM with thiol-reactive maleimide reagents and functional cysteine insertion hRFC mutants to verify the topological structure for TMDs 7–12 predicted by computer hydropathy analysis. Patterns of reactivity for biotin maleimide and protection by stilbenedisulphonate maleimide for residues localized in the connecting loops for TMDs 7–8, 9–10 and 11–12 were consistent with their exofacial orientations, and labelling of A332C in the TMD 8–9 and TMD 10–11 loop regions could be achieved only by permeabilization with SLO, consistent with their cytosolic orientations.

As these studies were being completed, a related paper was published using similar methods to determine the topology of the hamster RFC [36]. Findings include extracellular orientations for positions 46 (TMD 1–2 loop), 179 (TMD 5–6), 300 (TMD 7–8), 355 (TMD 9–10) and 430 (TMD 11–12), and intracellular orientations for positions 152 (TMD 4–5), 224 (TMD 6–7) and 475 (C-terminus) [36]. While these results are consistent with our findings for TMDs 7 and 8, 9 and 10, and 11 and 12, the orientations of the loops connecting TMDs 8 and 9 and 10 and 11, identified herein as intracellular, were not established.

In combination with previous findings of N-glycosylation at Asn-58 of hRFC, and the previous results from HA-insertional and scanning glycosylation mutagenesis studies, our results strongly argue for a 12 transmembrane structure for the hRFC protein with cytosolic-facing N- and C-termini and an internal TMD 6–7 loop domain. Future studies will focus on further delineating the TMD loop junctions, and explore the critical structural and functional features of the hRFC protein, including identification of the particular domains and amino acids that directly contribute to substrate binding and membrane traverse of anionic folate and antifolate substrates. These studies should be facilitated by the availability of a functional cysteine-less hRFC [25] and an established topological structure for the carrier.

We thank Dr Wayne Flintoff for his gift of the MtxRIIOua^{R}2-4 CHO cell line. This study was supported by grant CA53535 from the National Cancer Institute, National Institutes of Health, Bethesda, MD, U.S.A.

REFERENCES

1 Matherly, L. H. and Goldman, I. D. (2003) Membrane transport of folates. Vitamins Hormones **66**, 403–456
2 Sirotnak, F. M. and Tolner, B. (1999) Carrier-mediated membrane transport of folates in mammalian cells. Annu. Rev. Nutr. **19**, 91–122
3 Goldman, I. D. and Matherly, L. H. (1985) The cellular pharmacology of methotrexate. Pharmacol. Ther. **28**, 77–102
4 Jansen, G. (1999) Receptor- and carrier-mediated transport systems for folates and antifolates: exploitation for folate-based chemotherapy and immunotherapy. In Antifolate Drugs in Cancer Therapy (Jackman, A. L., ed.), pp. 293–322, Humana Press, Totowa
5 Schuetz, J. D., Matherly, L. H., Westin, E. H. and Goldman, I. D. (1988) Evidence for a functional defect in the translocation of the methotrexate transport carrier in a methotrexate resistant murine L1210 leukemia cell line. J. Biol. Chem. **263**, 9840–9847
6 Wong, S. C., McQuade, R., Proefke, S. A. and Matherly, L. H. (1997) Human K562 transfectants expressing high levels of reduced folate carrier but exhibiting low transport activity. Biochem. Pharmacol. **53**, 199–206
7 Wong, S. C., Zhang, L., Witt, T. L., Proefke, S. A., Bhushan, A. and Matherly, L. H. (1999) Impaired membrane transport in methotrexate-resistant CCRF-CEM cells involves early translation termination and increased turnover of a mutant reduced folate carrier. J. Biol. Chem. **274**, 10388–10394
8 Jansen, G., Mauritz, R., Drori, S., Sprecher, H., Kathman, I., Bunni, M., Priest, D. G., Noordhuis, P., Schornagel, J. H., Pinedo, H. M. et al. (1998) A structurally altered human reduced folate carrier with increased folic acid transport mediates a novel mechanism of antifolate resistance. J. Biol. Chem. **273**, 30189–30198
9 Gong, M., Yess, J., Connolly, T., Ivy, S. P., Ohnuma, T., Cowan K. H. and Moscow, J. A. (1997) Molecular mechanism of antifolate transport deficiency in a methotrexate resistant MOLT-3 human leukemia cell line. Blood **89**, 2494–2499
10 Sadlish, H., Murray, R. C., Williams, F. M. R. and Flintoff, W. F. (2000) Mutations in the reduced folate carrier affect protein localization and stability. Biochem. J. **346**, 509–516
11 Sirotnak, F. M., Moccio, D. M., Kelleher, L. E. and Goutas, L. J. (1981) Relative frequency and kinetic properties of transport-defective phenotypes among methotrexate resistant L1210 clonal cell lines derived *in vivo*. Cancer Res. **41**, 4442–4452
12 Goldman, I. D. and Zhao, R. (2002) Molecular, biochemical, and cellular pharmacology of pemetrexed. Semin. Oncol. **29**, 3–17
13 Zhang, L., Taub, J. W., Williamson, M., Wong, S. C., Hukku, B., Pullen, J., Ravindranath, Y. and Matherly, L. H. (1998) Reduced folate carrier gene expression in childhood acute lymphoblastic leukemia: relationship to immunophenotype and ploidy. Clin. Can. Res. **4**, 2169–2177
14 Gorlick, R., Goker, E., Trippett, T., Steinherz, P., Elisseyeff, Y., Mazumdar, M., Flintoff, W. F. and Bertino, J. R. (1997) Defective transport is a common mechanism of acquired methotrexate resistance in acute lymphoblastic leukemia and is associated with decreased reduced folate carrier expression. Blood **89**, 1013–1018
15 Guo, W., Healey, J. H., Meyers, P. A., Ladanyai, M., Huvos, A. G., Bertino, J. R. and Gorlick, R. (1999) Mechanisms of methotrexate resistance in osteosarcoma. Clin. Can. Res. **5**, 621–627
16 Wong, S. C., Proefke, S. A., Bhushan, A. and Matherly, L. H. (1995) Isolation of human cDNAs that restore methotrexate sensitivity and reduced folate carrier activity in methotrexate transport-defective Chinese hamster ovary cells. J. Biol. Chem. **270**, 17468–17475
17 Prasad, P. D., Ramamoorthy, S., Leibach, F. H. and Ganapathy, V. (1995) Molecular cloning of the human placental folate transporter. Biochem. Biophys. Res. Commun. **206**, 681–687
18 Williams, F. M. and Flintoff, W. F. (1995) Isolation of a human cDNA that complements a mutant hamster cell defective in methotrexate uptake. J. Biol. Chem. **270**, 2987–2992
19 Moscow, J. A., Gong, M., He, R., Sgagias, M. K., Dixon, K. H., Anzick, S. L., Meltzer, P. S. and Cowan, K. H. (1995) Isolation of a gene encoding a human reduced folate carrier (RFC1) and analysis of its expression in transport-deficient, methotrexate-resistant human breast cancer cells. Cancer Res. **55**, 3790–3794
20 Hofmann, K. and Stoffel, W. (1993) TMbase-a database of membrane spanning proteins segments. Biol. Chem. Hoppe-Seyler **347**,166–171
21 Wong, S. C., Zhang, L., Proefke, S. A. and Matherly, L. H. (1998) Effects of the loss of capacity for N-glycosylation on the transport activity and cellular localization of the human reduced folate carrier. Biochim. Biophys. Acta **1375**, 6–12

22 Ferguson, P. L. and Flintoff, W. F. (1999) Topological and functional analysis of the human reduced folate carrier by hemagglutinin epitope insertion. J. Biol. Chem. **274**, 16269–16278
23 Liu, X. Y. and Matherly, L. H. (2002) Analysis of membrane topology of the human reduced folate carrier protein by hemagglutinin epitope insertion and scanning glycosylation insertion mutagenesis. Biochim. Biophys. Acta **1564**, 333–342
24 Popov, M., Tam, L. Y., Li, J. and Reithmeier, R. A. (1997) Mapping the ends of transmembrane segments in a polytopic membrane protein. Scanning N-glycosylation mutagenesis of extracytosolic loops in the anion exchanger, Band 3. J. Biol. Chem. **272**, 18325–18332
25 Cao, W. and Matherly, L. H. (2003) Characterization of a Cysteine-less human reduced folate carrier: localization of a substrate binding domain by cysteine-scanning mutagenesis and cysteine accessibility methods. Biochem. J. **374**, 27–36
26 Fry, D. W., Yalowich, J. C. and Goldman, I. D. (1982) Rapid formation of poly-gamma-glutamyl derivatives of methotrexate and their association with dihydrofolate reductase as assessed by high pressure liquid chromatography in the Ehrlich ascites tumor cell *in vitro*. J. Biol. Chem. **257**, 1890–1896
27 Flintoff, W. F., Davidson, S. V. and Siminovitch, L. (1976) Isolation and partial characterization of three methotrexate-resistant phenotypes from Chinese hamster ovary cells. Somatic Cell Genet. **2**, 245–261
28 Lowry, O. H., Rosebrough, N. J., Farr, A. L. and Randall, R. J. (1951) Protein measurement with the Folin phenol reagent. J. Biol. Chem. **193**, 265–275
29 Matherly, L. H., Czajkowski, C. A. and Angeles, S. M. (1991) Identification of a highly glycosylated methotrexate membrane carrier in K562 human erythroleukemia cells up-regulated for tetrahydrofolate cofactor and methotrexate transport. Cancer Res. **51**, 3420–3426
30 Laemmli, U. K. (1970) Cleavage of structural proteins during the assembly of the head of bacteriophage T4. Nature (London) **227**, 680–685
31 Matsudaira, P. (1987) Sequence from picomole quantities of proteins electroblotted onto polyvinylidene difluoride membranes. J. Biol. Chem. **262**, 10035–10038
32 Bhakdi, S., Weller, U., Walev, I., Martin, E., Jonas, D. and Palmer, M. (1993) A guide to the use of pore-forming toxins for controlled permeabilization of cell membranes. Med. Microbiol. Immunol. **182**, 167–175
33 Clark, S. F., Martin, S., Carozzi, A. J., Hill, M. M. and James, D. E. (1998) Intracellular localization of phosphatidylinositide 3-kinase and insulin receptor substrate-1 in adipocytes: potential involvement of a membrane skeleton. J. Cell Biol. **140**, 1211–1225
34 Loo, T. W. and Clarke, D. M. (1995) Membrane topology of a cysteine-less mutant of human P-glycoprotein. J. Biol. Chem. **270**, 843–848
35 Grunewald, M., Bendahan, A. and Kanner, B. I. (1998) Biotinylation of single cysteine mutants of the glutamate transporter GLT-1 from rat brain reveals its unusual topology. Neuron **21**, 623–632
36 Flintoff, W. F., Williams, F. M. R. and Sadlish, H. (2003) The region between transmembrane domains 1 and 2 of the reduced folate carrier forms part of the substrate binding pocket. J. Biol. Chem. **278**, 40867–40876

Received 26 August 2003/4 November 2003; accepted 6 November 2003
Published as BJ Immediate Publication 6 November 2003, DOI 10.1042/BJ20031288